Positron annihilation study of density fluctuations in amorphous poly(ethylene terephthalate) films in terms of quasispinodal decomposition

Tong Xu,[1] Yuezhen Bin,[1] Nikolay Djourelov,[2] Takenori Suzuki,[2] and Masaru Matsuo[1,*]
[1]*Department of Textile and Apparel Science, Faculty of Human Life and Environment, Nara Women's University, Nara 630-8263, Japan*
[2]*High Energy Accelerator Research Organization (KEK), 1-1 Oho, Tsukuba, Ibaraki, 305-0032, Japan*
(Received 6 September 2004; published 23 February 2005)

Positron annihilation lifetime spectroscopy was applied to study poly(ethylene terephthalate). Changes in the positronium yield as a function of the temperature and as a function of the elapsed experiment time at predetermined constant temperatures were measured. The long-lived component was due to ortho-positronium (o-Ps) pick-off annihilation, and the temperature dependences of the o-Ps lifetime (τ_3) and the corresponding intensity (I_3) were in good agreement with the molecular mobility of the polymer chain segments. The peak positions of the β (74 °C) and γ (−66 °C) dispersions obtained by dynamic mechanical measurements were in good correlation with the first and second transitions of τ_3. The mechanical dispersion and the first transition appeared at around 70 °C, while the dispersion and the second transition appeared around −66 °C. The curves of τ_3 and I_3 as a function of the elapsed experiment time can be divided into three stages: stage I, where τ_3 and I_3 were maintained constant; stage II, where τ_3 and I_3 tended to decrease; and stage III, where τ_3 and I_3 tended to keep constant again. The higher was the annealing temperature, the shorter became the periods of stages I and II. This result was similar to that obtained by using time-resolved light scattering. Furthermore, time-resolved x-ray diffraction indicated no existence of crystallites in stage II. Thus, it turned out that the decreases of τ_3 and I_3 with elapsed time in stage II corresponded to the molecular ordering arising due to the density fluctuations of the amorphous phase associated with quasispinodal decomposition.

DOI: 10.1103/PhysRevB.71.075204 PACS number(s): 61.41.+e, 82.35.Lr, 78.70.Bj, 36.10.Dr

I. INTRODUCTION

The growth of polymer crystals has been well established in the literature, and there are reliable theories to predict the kinetics of crystallization.[1–10] Although most of these studies have been concentrated on observations of crystal growth processes, the initiation of the crystallization or nucleation step remains somewhat of a mystery. Recently, there is an increasing body of evidence that polymer crystallization, in general, may be assisted by the formation on an intermediate metastable state of poly(ethylene terephthalate) (PET), which can provide amorphous films. Geil[9] has reported an amorphous structure having nodules of about 100 Å in diameter based on observations of low-temperature annealed PET by transmission electron microscopy. Herglotz[10] has found that crystalline PET films annealed from the glassy state have a supermolecular structure with a size of about 100 nm. These experimental results indicated that a long-range structure is formed during the annealing processes.

Apart from the above concept, Imai[8] investigated the kinetics during the induction period of PET crystallization by means of depolarized light scattering. They pointed out that this period is associated with spinodal decomposition (SD) caused by orientation fluctuations of chain segments in terms of the concept concerning the transformation from the isotropic to nematic phase proposed by Doi *et al.*[11]

According to a recent PET investigation by Xu *et al.*,[12] the logarithm of the scattered intensity against time increased linearly after several tens of minutes when the amorphous film had been put into a hot oven at the desired temperature, and an incident beam of a He-Ne gas laser had been directed to the film. This increasing tendency was apparently in accordance with the concentration fluctuation of linear theories of spinodal decomposition originally proposed by Cahn and Hilliard[13,14] for small molecules, and modified by de Gennes[15] for a polymer system that describes the initial stage in the phase-separation process. The scattering maximum as a function of time remained almost constant at the same scattered vector, characterizing the early stage of SD. Surprisingly, the above phenomenon indicates that the observation scale of the density fluctuations associated with the driving force of the crystallization process was several hundred nanometers. Such a behavior is quite different from the density fluctuations at small scales detected by x-ray diffraction and scattering.[6,7] Based on the behavior, the apparent spinodal temperatures could be estimated from the dynamics measured as a function of the temperature for undrawn and drawn PET films. The growth rate maximum of the density fluctuation was independent of the scattered vector (q), and the maximum peak of the scattered intensity increased with time, but was independent of q in the early stage of SD. Of course, the scattered intensity hardly increased at the SD temperature. To give more conclusive evidence for our concept, in this paper, further analysis using positron annihilation lifetime (PAL) spectroscopy is done in terms of the local molecular orientation, leading to a density fluctuation of the PET amorphous state around the SD temperature.

The PAL technique is a powerful tool to study the free volume of polymers,[16–23] and usually the lifetime spectrum is resolved into three components with lifetimes of τ_1, τ_2, and

τ_3. The longest lifetime (τ_3) which is called the third long-lived position annihilation,[11] is on the scale of 10^{-9} s, and is related to the state and the chemical reaction of positronium (Ps).[21] In polymeric materials, the third component is due to the pick-off annihilation of o-Ps, localized in free-volume holes, and is the one carrying structure information.[22] Recently, PAL spectroscopy has been widely applied to study the size distribution of intermolecular spaces, relaxation behavior, and thermal properties.[17,24,25] In the present work, Ps formation in PET amorphous films was studied as a function of the temperature and time when the film was subjected to a rapid temperature jump to desired temperatures. The analysis was pursued by comparing the results measured by using PAL spectroscopy with several results measured using small-angle light scattering (SALS), dynamic mechanical measurements, and wide-angle x-ray diffraction (WAXD). The results enable one to extensively understand the temperature and time dependences of the density fluctuations of the amorphous state based on quasispinodal decomposition.

II. EXPERIMENTAL SECTION

A. Preparation of specimens

The PET films used in this study were furnished by Toyobo Industries, Inc. The number-average molecular weight ($\overline{M}_n$) was 15 000, and the polydispersity ($\overline{M}_w/\overline{M}_n$) was 3.47, where $\overline{M}_w$ is a weight-average molecular weight. The density of the amorphous PET film was ca. 1.335 g cm^{-3}, which was the same specimen as that used in previous studies.[12,28] The film thickness was about 200 μm. The glass transition temperature was 72.3 °C, estimated by differential scanning calorimetry (DSC).[28]

B. Measurements

1. Positron annihilation lifetime spectroscopy

The PAL experiments were conducted using two conventional fast-fast coincidence systems having a time resolution of 300 ps full width at half maximum. The sample chamber of the first system was combined with a closed–cycle He compressor (CW303), made by Iwatani Co. Ltd., ensuring measurements in a vacuum in the temperature range of −240–100 °C. The second system was combined with a heating device, and the PAL measurements were performed in a nitrogen atmosphere in the temperature range of 20–130 °C. Each spectrometer was composed of two plastic scintillators (40 mm $\phi\times$40 mm Pilot-U mounted on Hamamatsu H1949 photomutipliers), two differential constant-fraction discriminators (ORTEC 583) (one for start signals from 1.27 MeV γ rays, and the other one for stop signals from 0.511 Mev annihilation γ rays), a time-to-amplitude converter (ORTEC 4570), and a multi channel analyzer with a 1024 conversion gain (EG&G/ORTEC 919E). The positron source used was prepared by depositing ca. 1.1 MBq (30 μCi) of aqueous ^{22}NaCl on a Kapton foil of 7 μm thickness and 10×10 mm^2 area. The source was further sealed in a 3 μm Mylar foil and then sandwiched by two identical samples. The counting rate of the system was about 1×10^6 events in 1 h. The PAL spectra were analyzed by the POSITRONFIT program,[26] and no source correction was applied. The additional Mylar foil gave a permanent contribution to I_3 of ~0.5%, which does not influence the present discussion.

2. Viscoelastic measurement

The complex dynamic tensile modulus was measured at 10 Hz over a temperature range from −145 to 99 °C by using a viscoelastic spectrometer (VES-F) obtained from Iwamoto Machine Co. Ltd. The length of the specimen between the jaws was 40 mm and the width was 2 mm. During measurements, the film was subjected to a static tensile strain in order to place the sample in tension during the axial sinusoidal oscillation, which had a peak deformation of 0.05–0.1%. The complex dynamic modulus was measured by imposing a small dynamic strain to assure a linear viscoelastic behavior of the specimen.[27]

3. Light scattering measurement

The *in situ* time-revolved scattered intensity (depolarization condition) was measured by using a 632.8 nm He-Ne laser. To measure the time dependence of the scattered intensity, photodiodes were set at fixed scattering angles. The specimens were subjected to a rapid temperature jump to the desired temperatures. The time required to achieve the equilibrium temperature is ca. 1 min. The change in the angular distribution of the scattered intensity with time was measured when the fixed specimen was annealed isothermally in a temperature-controlled cell.

4. Wide-angle x-ray diffraction measurement

X-ray measurements were carried out with a 12 kW rotating-anode x-ray generator (Rigaku RDA-rA) operated at 200 mA and 40 kV. The intensity was detected with a curved position-sensitive proportional counter in an equatorial direction. The x-ray source was monochromatized to Cu $K\alpha$ radiation with a platelike graphite monochromator. The scattering intensity with time was measured in the range of 5°–35° (twice the Bragg angle, $2\theta_B$). The detailed method is described elsewhere.[28]

5. Crystallinity

The weight crystallinity (X_c) of PET films was calculated from the density measured by a pycnometer in a mixture of carbon tetrachloride and *n*-heptane as a medium, using 1.455 and 1.335 g cm^{-3} as the densities of the crystal and amorphous phases, respectively,[29]

$$X_c = \frac{\rho_c(\rho-\rho_c)}{\rho(\rho_c-\rho_a)}\times 100\% \quad (1)$$

where ρ is the density of the specimen and ρ_c and ρ_a are the densities of the crystal and amorphous phases, respectively.

III. RESULTS AND DISCUSSION

Figure 1 shows the temperature dependence of the storage modulus (E') and the loss modulus (E'') at a frequency of

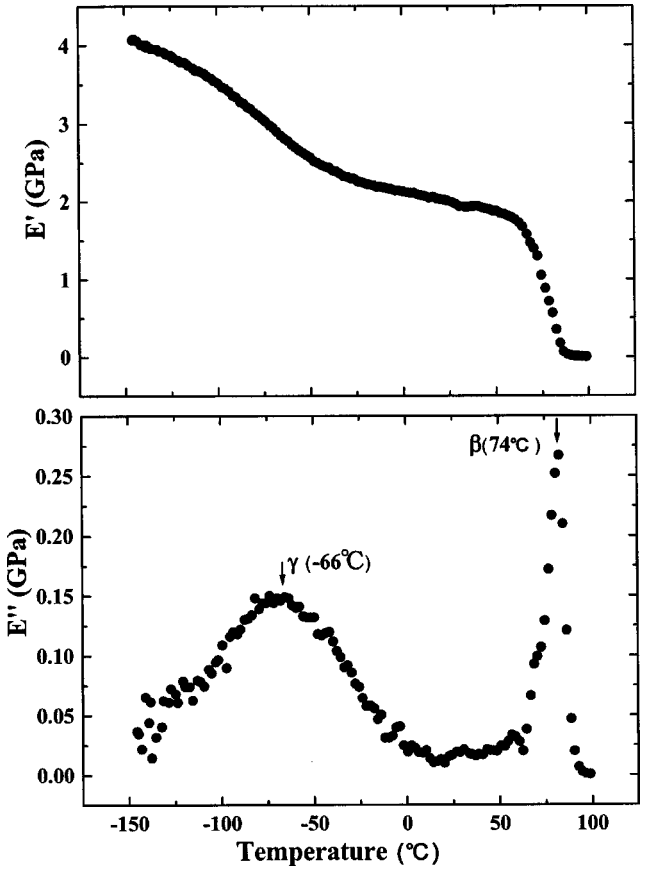

FIG. 1. Temperature dependence of the storage (E') and loss moduli (E'') for undrawn PET film measured at 10 Hz.

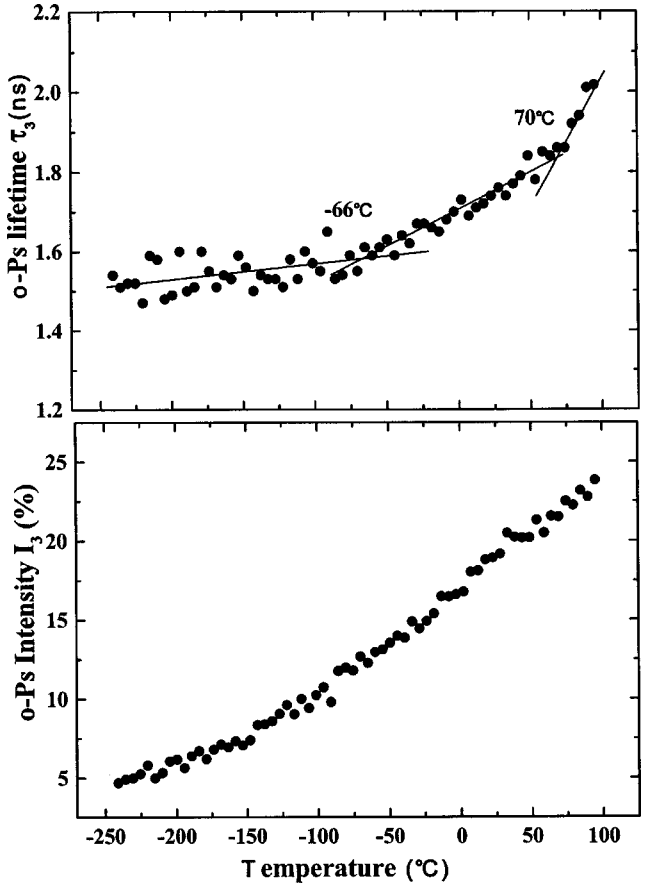

FIG. 2. Temperature dependence of the o-Ps lifetime and its intensity in an amorphous PET film. The heating rate is 5 °C/h.

10 Hz for PET film. E' decreases with increasing temperature. This tendency is the usual manner, as has generally been observed for polymers. The curve of E'' has two peaks: a very sharp peak at around 74 °C corresponding to the β dispersion, and a very broad peak at around −66 °C, corresponding to the γ dispersion. The results are similar to those by Illers and Breuer,[30] which were reported for the temperature dependence of the shear modulus (G') and the loss modulus (G'') with a torsion pendulum at a constant frequency of 1 cycle/s in the temperature range between −180 and 260 °C. A very broad peak of E'' appeared at a mean value of about −66 °C, which was also reported for G''. Such low-temperature processes have been confirmed for many other polymers, but usually lead to contributions from much sharper peaks. This suggests that the mechanism of this low-temperature process in PET is a very complicated one. The broad peak of E'' is certainly built up from two or more closely adjacent peaks, belonging to the motions of different groups or groups with different steric or energetic interactions. According to NMR experiments by Ward *et al.*,[31] there are hindered rotations of methylene groups below the glass transition temperature, which presumably also occur within the crystalline regions. On the other hand, their dielectric measurements revealed a participation of the COO groups. Accordingly, the contribution of the methylene groups to the E'' peak will mainly be at temperatures below ca. −120 °C, while that of the COO groups may be expected at higher temperatures. Based on the same concept, Zhuang and Zuo[32] reported a transition between the *cis* and *trans* configurations of the ester groups caused by the dielectric absorption process.

Figure 2 shows the τ_3 and I_3 temperature dependences for the amorphous PET film. The heating rate is 5 °C/h. Although the o-Ps lifetime has been successfully correlated to the size of the free-volume holes in polymers, its intensity has been found to be influenced by many factors, such as the temperature,[33,34] positron irradiation,[35,36] electric field,[37] and polar group.[38] Under proper conditions, I_3 might be used to relate to the fraction of the free volume in polymers.

The error bars in Fig. 2 have been omitted to make the picture more readable. With increasing the temperature, I_3 and τ_3 increase. In this figure, two transitions for the amorphous PET film are observed. The NMR measurements by Ward[31] clearly revealed that above the β-dispersion temperature, both the benzene ring and the methylene group protons undergo considerable molecular motion. Since then, the β dispersion at 74 °C has been explained as a contribution from the glass transition (the β dispersion) associated with an increase in the free volume and the micro-Brownian motion of the chain segments starting at this temperature. Incidentally, the existence of the α dispersion associated with crystal relaxation was found as a small peak by Yoshihara *et al.*,[39] who found the existence of α dispersion by the peak separation of a nonsymmetrical broad dispersion. The peak

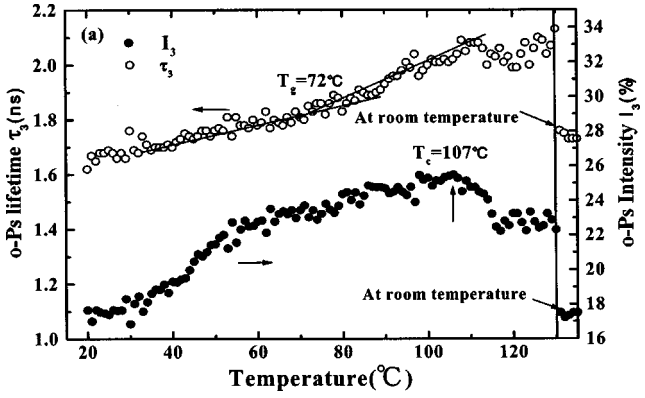

FIG. 3. Temperature dependence of the o-Ps lifetime and its intensity in an amorphous PET film.

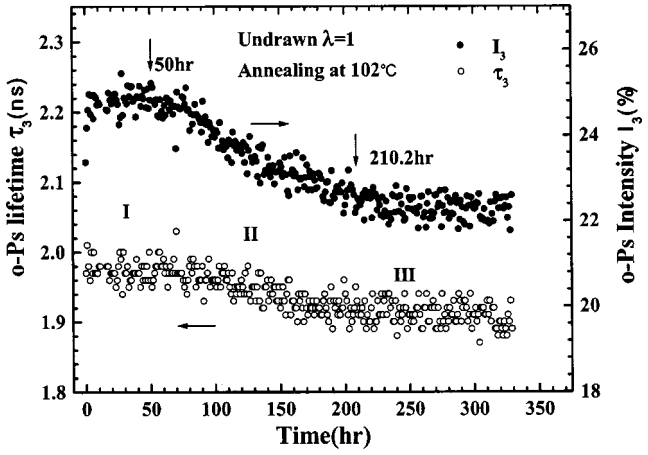

FIG. 4. Intensity of o-Ps, varying as a function of the elapsed time at 102 °C for undrawn amorphous PET film. The solid symbols are for the o-Ps intensity and the open symbols are for the corresponding o-Ps lifetimes.

appeared at a temperature close to the β dispersion. Here, we must emphasize that the α dispersion assigned by Illers and Breuer[30] and Zhuang and Zuo[32] corresponds to the β dispersion, and that the β dispersion corresponds to the γ dispersion discussed in this paper.

From the results shown in Figs. 1 and 2, it turns out that for amorphous PET films, the temperatures associated with the first and second transitions are in good agreement with those associated with the β and γ dispersions, respectively. As discussed above, the β-dispersion peak has been thought to be attributable to the glassy transition associated with the micro-Brawnian motion of local chain segments. However, the second transition of τ_3, as seen by PAL experiments, corresponds to the γ-dispersion peak associated with the local movement of COO groups. Incidentally, such a good correlation between mechanical dispersion and the transition points detected by PAL spectroscopy was also confirmed for ultradrawn polyethylene films.[25]

In condensed matter, Ps tends to localize in low-density parts of the sample, and the intrinsic o-Ps lifetime (142 ns) is reduced to several nanoseconds. This is caused by o-Ps annihilation with one electron, picked off from the surrounding matter. The value of τ_3 for the pick-off process depends on the size (R) of the free-volume hole at which o-Ps is trapped. According to a quantum-mechanical model proposed by Tao[16] and Eldrup *et al.*[23] the longest lifetime (τ_3) can be correlated with the average radius of the free-volume holes in the polymer matter. Nakanishi and Jean[40] derived the following semiempirical equation:

$$\tau_3 = 0.5\left[1 - \frac{R}{R+1.66} + \frac{1}{2\pi}\sin\left(\frac{2\pi R}{R+1.66}\right)\right]^{-1} \qquad (2)$$

where τ_3 is the o-Ps lifetime expressed in nanoseconds, R is the average radius of the spherical well expressed in angstroms, and 1.66 Å is an empirical constant.

The free volume in Å^3 corresponds to the hole volume $V_f=(4/3)\pi R^3$, and the average size of free-volume holes (hole radius R) can be calculated by Eq. (2) from the value of τ_3. Figure 3 shows the τ_3 and I_3 temperature dependences for an amorphous PET film. The heating rate is 2 °C/h. The error bars in Fig. 3 have also been omitted because the error is very small. The transition temperatures of τ_3 and I_3 are ca. 107 and ca. 72 °C, respectively. From ca. 72 °C, τ_3 changed its rising slope, and began to increase more rapidly. Considerable changes in the polymer amorphous parts occur during their crystallization. These changes, especially the free-volume structure, have been studied by PAL methods.[22,38]

The intensity of the o-Ps component in the annihilation spectra is often connected with the number of free-volume holes.[41–43] In Fig. 3, the relative intensity of I_3 increases from ca. 18% to 25% when the temperature increases from room temperature to ca. 107 °C; this can be explained by an increase in the number of holes. Beyond ca. 107.3 °C, the I_3 value dropped immediately to ca. 23%, and then stayed constant. Generally, I_3 is affected by many factors, as shown in the beginning of this section. From the fact that this temperature coincides with the spinodal temperature of 108 °C,[12] which was observed by a time-resolved light scattering technique, it is reasonable to connect this drop of I_3 to the molecular ordering by density fluctuations due to quasispinodal decomposition. Ps atoms tend to be localized in the disordered parts (low-density parts) of a polymer matrix, and in semicrystalline polymers Ps is localized in the amorphous regions and crystalline-amorphous interface.[44] Therefore, a correlation between the crystallinity of the samples and the o-Ps formation probability is often observed.[45] The rapid drop at 107.3 °C is not the result of crystallization. Because of the measurement by time-resolved light scattering, the drop may suggest the possibility of molecular ordering (densification), which reduces the free-volume spaces available for Ps and leads to a decrease in I_3. Of course, molecular ordering does not cause the formation of crystallites, but the formation of a local orientation of amorphous chains. Actually, the spinodal temperature by time-resolved light scattering was confirmed to be ca. 108 °C.[12]

Figure 4 shows the time dependence of τ_3 and I_3 at 102 °C for an amorphous PET film. The temperature jump in 10 min was from room temperature up to 102 °C, and was then kept at 102 °C. It is obvious that the curves can be divided into three stages: stage I (ca. 0–50 h), where τ_3 and I_3 of o-Ps remain constant; stage II (ca. 50–210 h), where τ_3

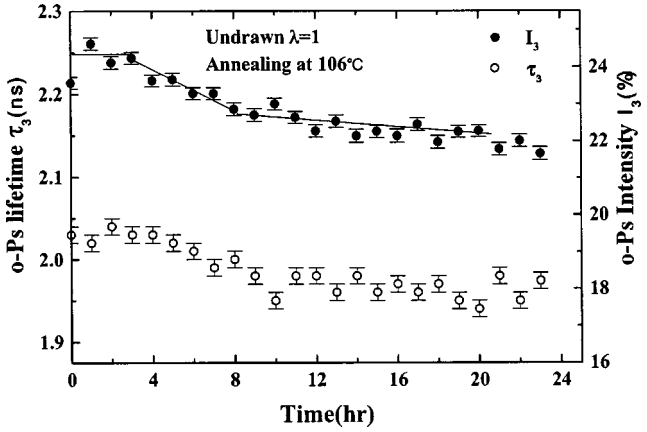

FIG. 5. Intensity of o-Ps, varying as a function of the elapsed time at 106 °C for undrawn amorphous PET film. The solid symbols are for the o-Ps intensity and the open symbols are for the corresponding o-Ps lifetimes.

and I_3 tend to decrease with the elapsed time; and stage III (after 210 h), where τ_3 and I_3 remain constant again. Detailed observation, however, reveals a very slight decrease of I_3 in stage III. Such a classification is similar to that already observed by time-resolved light scattering,[12] which also suggests that the decrease in the time period from ca. 50 to 210 h can be attributed to the molecular ordering by density fluctuations.

Figure 5 shows the temperature dependence of τ_3 and I_3 at 106 °C for the amorphous PET film. The temperature jump was achieved in accordance with the same method as described in Fig. 4. The curves can also be classified according to three stages.: stage I (0–3 h) and stage II (3–10 h) become shorter than for those annealed at 102 °C. Furthermore, a clear gradual decrease in I_3 is observed in stage III, although τ_3 tends to remain constant again. Thus, it may be concluded that the higher the annealing temperature, the faster are the decreases of τ_3 and I_3. A similar tendency was also confirmed by time-resolved light scattering.[12]

Nakanishi *et al.*[46] observed that for poly(ether ether ketone) the o-Ps lifetime did not change with an increasing amount of crystallinity, but the o-Ps yield decreased linearly with increasing amount of crystallinity. Also Lind *et al.*[47] found a similar result for polypropylene where τ_3 changed very little with the amount of crystallinity. These results suggest that the decrease in both τ_3 and I_3 seen in stage II (Figs. 4 and 5) should not be ascribed to the crystallization process.

To give more conclusive evidence concerning the mechanism of the rapid drop of τ_3 and I_3, time-resolved light scattering and WAXD measurements were carried out, in order to compare with the results obtained by using PAL spectroscopy.

Figure 6(a) shows the change in $\ln(I)$ $q=2.77\times10^{-4}$ Å^{-1} and the appearance of a small-angle light scattering pattern under the cross-polarization condition, which is called the Hv scattering pattern, against time, measured for the amorphous PET film; q is the magnitude of the scattered vector, given by $q=(4\pi n/\lambda)\sin(\theta/2)$, where λ, θ, and n are the wavelength of light in the film, the scattered angle, and the refractive index, respectively. Figure 6(b) shows the density dependence on time and the corresponding crystallinity calculated by Eq. (1), assuming the intrinsic densities of the crystal and amorphous phases, as described in Sec. II. According to a previous paper,[12] the sample was heated rapidly up to 108 °C, corresponding to the spinodal temperature, and kept at the same temperature. The curve of the time dependence of the logarithm of the scattered intensity may be classified into three stages: the first stage (stage I), where

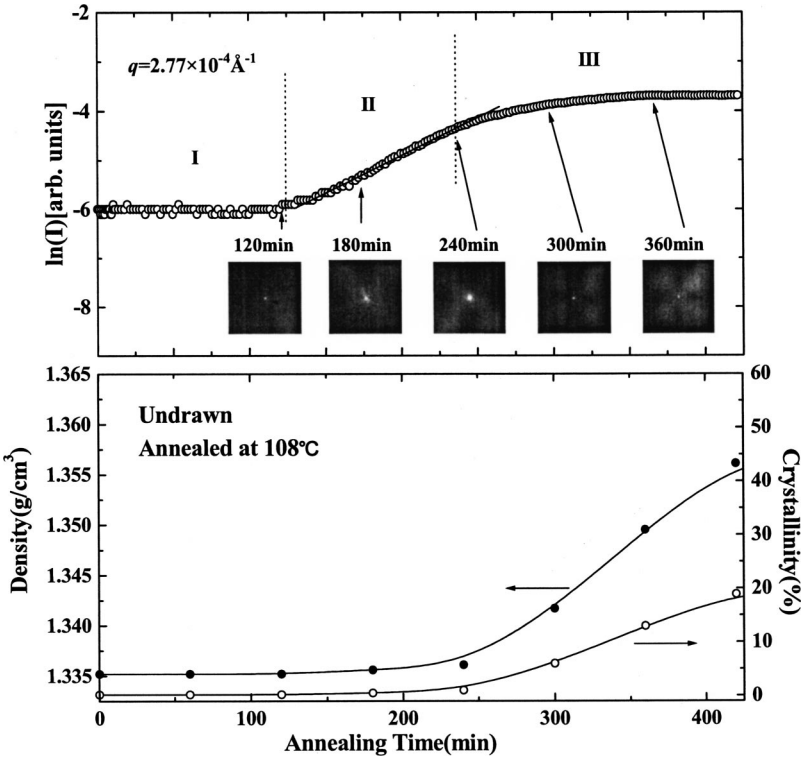

FIG. 6. (a) Change of $\ln(I)$ at $q=2.77\times10^{-4}$ Å^{-1} and the Hv SALS patterns with time. (b) Annealing-time dependence of the crystallinity and the density of undrawn amorphous PET.

the scattered intensity hardly changes with time; the second stage (stage II), where the intensity increases linearly; and the third stage (stage III), where the intensity starts to deviate from a linear relationship, and tends to level off. It has been reported that stage I corresponds to a limited time scale when the average length of the rigid segments attains a critical value, given by a theory[48] proposed by Shimada, Doi, and Okano, and is assigned to a process where the polymer chain segments begin to partially change the inconformation. As for amorphous PET films, it has been reported[7,49] that the internal rotation of the ethylene groups begins to be allowed due to the release from the frozen state, and the *trans* form is preferred to the *gauche* one to assure a more stable state when the film is annealed above the glass transition temperature. In a previous paper,[12] it was postulated that the conformational changes and the lengths of the rigid segments of the polymer chains increase in stage I. However, density fluctuations hardly occur in this stage, since the scattered intensity hardly increases at this time. This means that in stage I, the average length of the rigid segments does not attain a critical value. Judging from the similar time dependence of τ_3 and I_3 in Figs. 4 and 5, stage I is also thought to be the period of change of conformation and rigidity of the chain segments as described above.

When the critical length is achieved, the isotropic amorphous state becomes unstable, indicating that density fluctuations occur by spinodal decomposition. Actually, in stage II, logarithmic plots of the scattered intensity of $\ln(I)$ increase linearly with time, and the behavior is similar to the initial stage of phase separation of isotropic amorphous polymer blends by spinodal decomposition.[49–51] In a previous paper,[12] similar experiments were carried out by rapid temperature jumps from room temperature to the desired temperature ($\geqslant$110 °C). The change in the scattered intensity against time after stage I was analyzed by using the following equation:

$$I(q,t) = I(q,t=0)\exp[2\ R(q)t] \tag{3}$$

where $I(q,t)$ is the scattered intensity at time t after initiation of the spinodal decomposition, and $R(q)$ is the growth rate of the density fluctuation, given as a function of q; $R(q)$ is given by

$$R(q) = -D_c q^2 \left\{ \frac{\partial^2 f}{\partial^2 \rho} + 2\kappa q^2 \right\} \tag{4}$$

where D_c is the translational diffusion coefficient of the amorphous chains of PET film, f is the free energy, ρ is the density of the PET film, and κ is the density-gradient energy coefficient defined by Cahn and Hilliard.[13,14] Another detailed observation characterizing the early stage of SD revealed that, in stage II, the scattered intensity measured at each time has a peak, and that the peak becomes sharper without changing the peak position. Analysis by spinodal decomposition supported results obtained by x-ray, DSC, and density observation.[12]

As shown in Fig. 6(a), the Hv scattering pattern showed an indistinct circular type in stage I indicating no existence of any superstructure detected at the wavelength level of a He-Ne gas laser. In stage II, Hv scattering patterns observed at 180 and 240 min showed four indistinct broad lobes. Such a pattern has been reported to be due to scattering from sheaflike structures[26,52] with large fluctuation of the optical axes. In the sheaflike structures, the optical axes correspond to the ordered aggregation of amorphous chains. Actually, the density was almost the same as the original sample, indicating no crystallization. With increasing time, plots of $\ln(I)$ vs time deviate from the straight line, and the corresponding Hv scattering (300 min) shows a four-leaf-clover-type pattern, indicating the existence of spherulites. The structural change from a sheaflike structure to spherulite is obviously attributed to the growth of crystallites. Actually, in this stage (the immediate stage from stage II to stage III), the density and the apparent crystallinity began to increase. With a further lapse of time, at 360 min (in stage III) the pattern becomes more distinct indicating an increase in the number of spherulites associated with a gradual development of crystallites. In other words, no rapid increase in density occurs in stage II.

Returning to Figs. 4 and 5, it can be seen that the time dependence of τ_3 and I_3 obtained by PAL spectroscopy exhibits three stages. Especially, the time intervals for the three stages in Fig. 5 are similar to those shown in Fig. 6, since the rapid temperature jumps are similar (106 and 108 °C). As for the results at 106 °C, the time periods of stage I, stage II, and stage III are from 0 to 3 h (180 min), from 3.5 h (210 min) to 7 h (420 min), and from 7 h (420 min) to even longer times. Judging from the 2 °C difference between the light scattering and the positron annihilation measurements, the three stages of positron annihilation obviously correspond to the three stages of light scattering. In Figs. 4 and 5, for stage II, fast decreases in I_3 and τ_3 are attributed to spinodal decomposition, while for stage III, a slight gradual decrease in I_3, but no change in τ_3 is attributed to crystallization because a polymer with different crystallinity usually shows changes only in I_3 based on PAL measurements. Accordingly, the decrease of τ_3 and I_3 at 107.3 °C in Fig. 3 is thought to be attributable to the local molecular orientation of amorphous chains, leading to density fluctuations associated with quasispinodal decomposition.

A question can arise as to how these microscopic changes such as free-volume hole size and the hole number can be correlated with light scattering results indicating that the observation scale of the density fluctuation is several thousand nanometers. This is due to the fact that a number of free volumes exist in the large-scale density fluctuation region and then the transition from the uniform amorphous region with random molecular chains (low-density region) to the ordered-amorphous-chain region (high-density region) is sensitive to the decrease in free-volume hole size and the decrease in the number of free volumes. Thus the transition reflects the decreases in I_3 and τ_3 with elapsing time, as shown in Figs. 4 and 5.

In order to facilitate understanding of more detailed information concerning thermal crystallization, the x-ray intensity distribution was measured as a function of time at a fixed

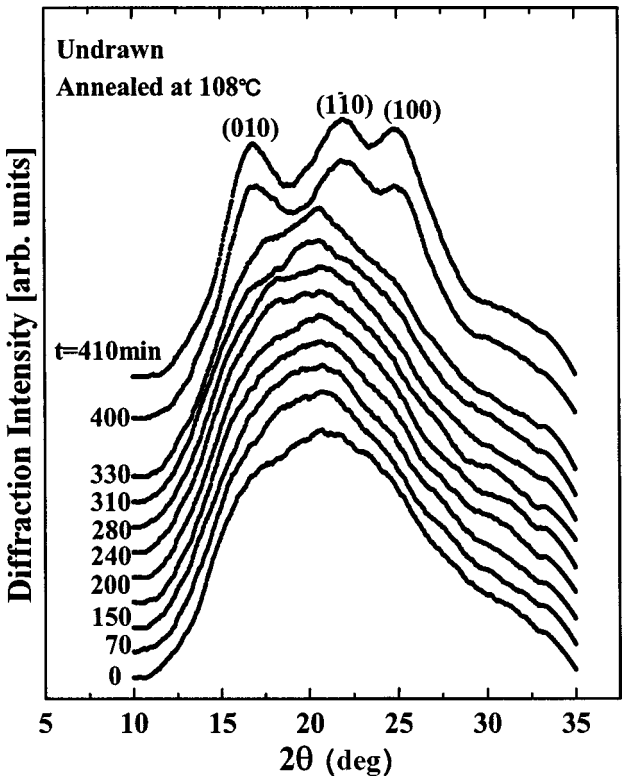

FIG. 7. Change in the WAXD profiles with time. The samples were isothermally annealed at the indicated temperature.

temperature. Figure 7 shows the change in the WAXD intensity profiles for amorphous PET specimens under an annealing process at 108 °C, corresponding to the spinodal temperature of the present amorphous PET film.[12] For convenience, the curves of the x-ray intensity are shifted along the intensity axis to clarify the time dependence of the intensity distribution. The time described in each x-ray curve indicates the beginning time of the accumulation of the x-ray intensity. The accumulation time was 5 min. The intensity distribution curve at 0 min denotes the accumulation intensity in the range from 0 to 5 min, since the accumulation time is 5 min. Compared with the time scale shown in Fig. 6, the indicated 0 and 70 min correspond to stage I in Fig. 6; 150, 200, and 240 min correspond to stage II. Furthermore, 280, 310, and 330 min correspond to the intermediate stage from the end of stage II to stage III, and 400 and 410 min correspond to stage III (as shown in Fig. 6). In stages I and II, the x-ray intensity diffraction still shows a smooth curve with a maximum of around $2\theta_B = 21°$ (θ_B is the Bragg angle), which is attributed to scattering from amorphous regions. When the light scattering measurement is beyond 280 min in Fig. 6(a), the corresponding x-ray intensity begins to split into several very weak diffraction peaks, indicating the beginning of crystallization. This means that stage II, which ensures the linear relationship of $\ln(I)$ with time, is independent of crystallization, because no existence of crystallites was detected by x-ray diffraction. The intensity curves show the reflections from the (010), (100), and $(1\bar{1}0)$ planes, when the annealing time is beyond 400 min. This indicates the appearance of large crystallites with the progression of crystallization.

The appearance of the diffraction peak indicates that the polymer-rich phase in the amorphous phase occurred because of the density fluctuation of amorphous chains associated with the local molecular orientation; subsequently, the unstable crystallites appear in the polymer-rich phase with further growth of the density fluctuations. Of course, the crystallization progresses with elapsing time.

Incidentally, when the specimen was heated by a rapid temperature jump to 102 °C and light scattering and x-ray measurements were done in the time range 0–8 h corresponding to the time range in Figs. 6 and 7, no change in light scattered intensity or x-ray diffraction intensity could be observed. This is due to the fact that 0–8 h is the time range corresponding to stage I with no change in τ_3 and I_3 (see Fig. 4). Incidentally, 8 h is the maximum time to pursue the light scattering experiment without any damage of He-Ne gas laser instrument. Anyway, this result, as a further confirmation, supports no density fluctuation of the amorphous phase in stage I.

Returning to Fig. 6, we confirmed no Hv scattering in stage I and confirmed an indistinct scattering with no azimuthal angle dependence of the pattern at the intermediate stage from the end of stage I to stage II. The pattern was of x type beyond 180 min. The Hv scattered intensity was much weaker than the corresponding Vv scattered intensity. Of course, the Vv scattering patterns was of circular type with no azimuthal angle dependence, indicating isotropic scattering. In such an initial stage showing a circular type of Hv pattern, we have[53]

$$I_{Vv} - \frac{4}{3} I_{Hv} = K \langle \eta^2 \rangle \int_0^\infty \gamma(r) \frac{\sin qr}{qr} r^2 \, dr \tag{5}$$

where $\langle \eta^2 \rangle$ is the mean-square polarizability fluctuation and $\gamma(r)$ is the corresponding correlation function. In the present study, the angular dependence of the scattered intensity is assumed to be a monotonically decreasing function. By using such a function, it is very difficult to obtain $\gamma(r)$ by a Fourier transformation with sufficient accuracy. The desired information could be extracted by assuming that the scattering over the entire angular range can be described by assuming Gaussians.[54] We thus have

$$\gamma(r) = \exp\left(- \frac{r^2}{a^2} \right). \tag{6}$$

Substituting Eq. (6)into Eq. (5)and performing the integration yields

$$\ln\left(I_{Vv} - \frac{4}{3} I_{Hv} \right) = \ln\left(\frac{16}{\lambda^4} \pi^{11/2} \langle \eta^2 \rangle a^3 \right) - \frac{a^2}{4} q^2. \tag{7}$$

The parameter a is the correlation length for estimating the extension of the inhomogeneities.[55] The amorphous phase becomes uniform when a takes an infinite value.

Figure 8 shows an example of the scattered intensity data plotted as the logarithm of the absolute Rayleigh ratio vs q^2 at the indicated time. The slope of the line allows a determination of the parameter a in Eq. (7).

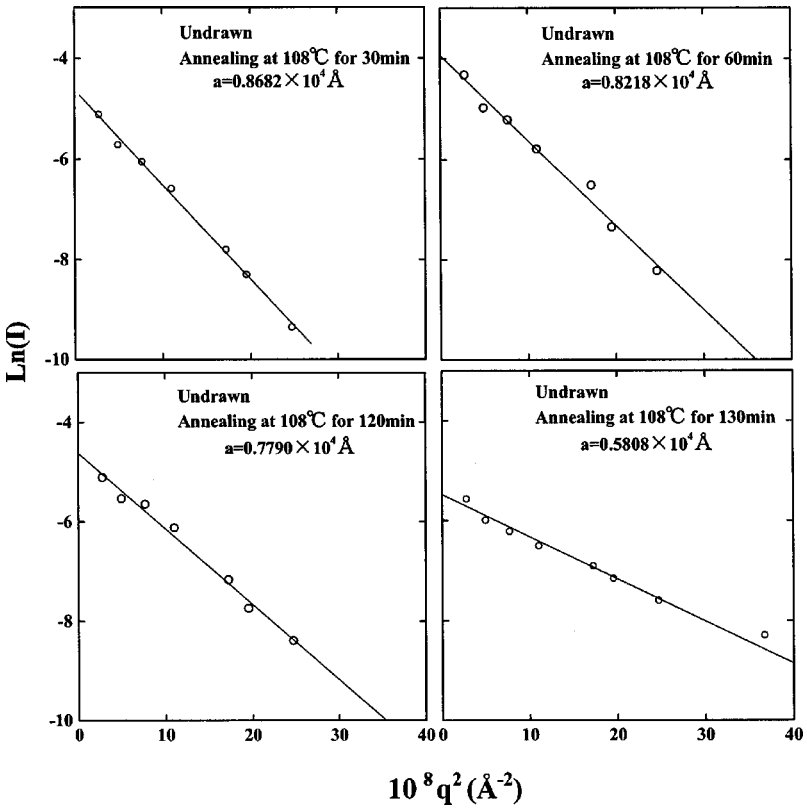

FIG. 8. Plots of $\ln(I)$ against q^2 for undrawn PET films.

Figure 9 shows $\gamma(r)$ curves recalculated by using the values of a. The profile of $\gamma(r)$ becomes sharper with increasing time. This indicates that the density fluctuation becomes more considerable with time; this tendency becomes significant at the beginning of stage II. That is, as for the profiles of $\gamma(r)$ at 30, 60, and 120 min, the profile becomes slightly sharper with increasing annealing time, reflecting that the conformational changes and the lengths of the rigid segments of the polymer chains increase in stage I. However, the profile at 130 min is much sharper than that at 120 min. The profile of $\gamma(r)$ at 130 min indicates the formation of a polymer-rich phase with local molecular ordering by density fluctuations characterizing the initial stage (stage II) of SD. Accordingly, the density fluctuation becomes more significant with elapsing time, and the ordered amorphous chains provide crystallization with regard to the growth of a stable crystal lattice detected by x-ray diffraction. Furthermore, it is worth mentioning that the polarized light scattering experiments provided a domain size with the local molecular orientation, which is much smaller than the wavelength of the He-Ne gas laser.

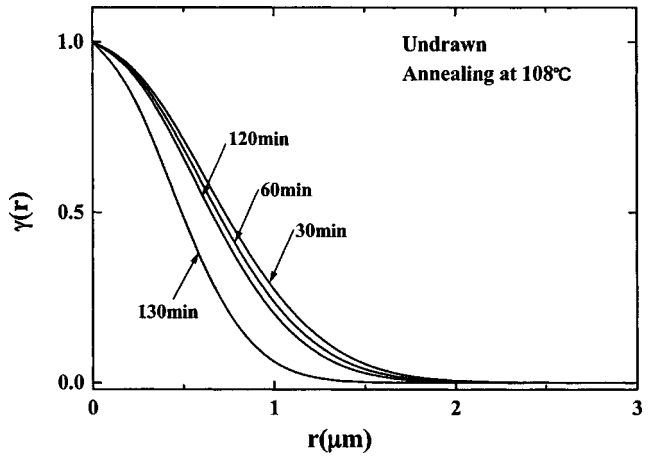

FIG. 9. Recalculated correlation function $[\gamma(r)]$ against the obtained r for undrawn PET films. The samples were annealed at 108 °C for 30, 60, 120, and 130 min, respectively.

IV. CONCLUSIONS

Positron annihilation lifetime spectroscopy has been applied to study poly(ethylene terephthalate) as a function of temperature, and as a function of the elapsed experiment time at predetermined constant temperatures. The temperature dependence of the o-Ps lifetime (τ_3) and the corresponding intensity (I_3) was in good correlation with the mechanical dispersions. The peak positions of the β (74 °C) and γ (−66 °C) dispersions, obtained by dynamic mechanical measurements, correspond to the first and second transitions of τ_3.

The curves of τ_3 and I_3 of o-Ps as a function of the elapsed experiment time can be divided into three stages: stage I, where τ_3 and I_3 are maintained constant; stage II, where τ_3 and I_3 decrease rapidly; and stage III, where τ_3 tends to remain constant, and I_3 gradually decreases. The higher the annealing temperature, the shorter stage I and stage II become and the more steeply does I_3 decrease in stage III. This result is similar to that obtained by using time-resolved light scattering. It thus turned out that the

higher the annealing temperature, the faster is the structural change. Furthermore, x-ray diffraction revealed no existence of crystallites in stages I and II. This means that the rapid drop of τ_3 and I_3 under the heating process is not due to crystallization, but due to the beginning of molecular ordering in the amorphous chains, leading to density fluctuations; namely, the temperature of the rapid drop of τ_3 and I_3 can be assigned to be equivalent to the quasispinodal temperature.

*Fax: 81-742-20-3462. Email address: m-matsuo@cc.nara-wu.ac.jp

[1] J. W. Gilmer, D. Wiswe, and H. G. Zachmann, Polymer **27**, 1391 (1986).
[2] R. Gehrhe, C. Reikel, and H. G. Zachmann, Polymer **30**, 1582 (1989).
[3] A. C. Middleton and R. A. Duckett, J. Appl. Polym. Sci. **79**, 1825 (2001).
[4] J. Radhakrishnan and A. Kaito, Polymer **42**, 3859 (2001).
[5] T. Asano and F. J. Baltá, Polymer **40**, 6475 (1999).
[6] M. Imai and K. Kaji, Phys. Rev. Lett. **71**, 4162 (1993).
[7] M. Imai, Phys. Rev. B **52**, 12 696 (1995).
[8] M. Imai, Phys. Rev. Lett. **71**, 4162 (1993).
[9] P. H. Geil, in *Order in the Amorphous State of Polymers*, edited byS. E. Keinath, R. L. Miller, and J. K. Rieke (Plenum, New York, 1987).
[10] H. K. J. Herglotz, J. Colloid Interface Sci. **75**, 105 (1980).
[11] M. Doi, T. Shimada, and K. Okano, J. Chem. Phys. **88**, 4070 (1988).
[12] T. Xu, Y. Bin, Y. Nakagaki, and M. Matsuo, Macromolecules **37**, 6985 (2004).
[13] J. W. Cahn, J. Chem. Phys. **42**, 93 (1965).
[14] J. W. Cahn and J. E. Hilliard, J. Chem. Phys. **28**, 258 (1958).
[15] P. G. de Gennes, J. Chem. Phys. **72**, 4756 (1980).
[16] S. J. Tao, J. Phys. Chem. **56**, 5499 (1977).
[17] D. M. Schrader and Y. C. Jean, *Positron and Positronium Chemistry: Studies in Physics and Theoretical Chemistry* (Elsevier, Amsterdam, 1988).
[18] Y. C. Jean, Microchem. J. **42**, 72 (1990).
[19] F. H. Maurer and M. Schmidt, Radiat. Phys. Chem. **58**, 509 (2000).
[20] M. McCullagh and Z. Yu, Macromolecules **28**, 6100 (1995).
[21] R. Zhang, Y. C. Wu, and H. Chen, Radiat. Phys. Chem. **68**, 481 (2003).
[22] M. Misheva, N. Djourelov, and I. Seganov, Acta Phys. Pol. A **99**, 429 (2000).
[23] M. Eldrup, D. Lightbody, and J. Sherwood, J. Chem. Phys. **63**, 51 (1981).
[24] O. E. Mogensen, *Positron Annihilation in Chemistry* (Springer, Berlin, 1995).
[25] M. Matsuo, L. Ma, M. Azuma, C. He, and S. Suzuki, Macromolecules **35**, 3059 (2002).
[26] P. Kirkegaard and M. Eldrup, Comput. Phys. Commun. **7**, 401 (1974).
[27] M. Matsuo, C. Sawatari, and T. Ohhata, Macromolecules **21**, 1317 (1988).
[28] T. Xu, Y. Bin, H. Kurosu, and M. Matsuo, Colloid Polym. Sci. **281**, 624 (2003).
[29] J. Brandrup, E. H. Immergut, and E. A. Grulke, *Polymer Handbook*, 4th ed. (John Wiley & Sons, New York, 1999).
[30] K. H. Illers and H. Breuer, J. Colloid Sci. **18**, 1 (1963).
[31] I. M. Ward, Trans. Faraday Soc. **56**, 648 (1960).
[32] H. Z. Zhuang and X. W. Zuo, J. Phys.: Condens. Matter **10**, 445 (1998).
[33] C. L. Wang, T. Hirade, and F. H. J. Maurer, J. Chem. Phys. **108**, 4654 (1998).
[34] Z. L. Peng, B. G. Olson, and J. D. McGervery, Polymer **40**, 3033 (1999).
[35] T. Suzuki, Y. Ito, and K. Kondo, Radiat. Phys. Chem. **60**, 535 (2001).
[36] C. He, T. Suzuki, and L. Ma, Phys. Lett. A **304**, 49 (2002).
[37] Y. Kobayashi, C. L. Wang, and K. Hirata, Phys. Rev. B **58**, 5384 (1998).
[38] T. Suzuki and C. He, Radiat. Phys. Chem. **66**, 161 (2003).
[39] N. Yoshihara, A. Fukushima, Y. Watanabe, A. Nakai, S. Nomura, and H. Kawai, Sen'i Gakkaishi **37**, 387 (1981).
[40] H. Nakanishi and Y. C. Jean, in *Positron and Positronium Chemistry*, edited by D. M. Schrader and Y. C. Jean (Elsevier Science, Amsterdam, 1988), pp. 159–192.
[41] Y. C. Jean, Mater. Sci. Forum **59**, 175 (1995).
[42] Y. Y. Wang, H. Nakanishi, Y. C. Jean, and T. Sandreczki, J. Polym. Sci., Part B: Polym. Phys. **28**, 1431 (1990).
[43] Y. Kobayashi, W. Zheng, and E. F. Meyer, Macromolecules **22**, 2302 (1989).
[44] G. Dlubek, J. Stejny, and T. Lüpke, J. Polym. Sci., Part B: Polym. Phys. **40**, 65 (2002).
[45] J. Serna, J. C. Abbe, and G. Duplatre, Phys. Status Solidi A **115**, 389 (1989).
[46] H. Nakanishi, Y. C. Jean, E. G. Smith, and T. C. Sandreczki, J. Polym. Sci., Part B: Polym. Phys. **27**, 1419 (1989).
[47] J. H. Lind, P. L. Jones, and G. W. Pearsall, J. Polym. Sci., Part A: Polym. Chem. **24**, 3033 (1986).
[48] T. Shimada, M. Doi, and K. Okano, J. Chem. Phys. **88**, 7181 (1988).
[49] H. Tadokoro, *Structure of Crystalline Polymers* (Wiley, New York, 1978).
[50] H. Yang, M. Shibayama, R. S. Stein, N. Shimizu, and T. Hashimoto, Macromolecules **19**, 1667 (1986).
[51] M. L. Wallach, J. Polym. Sci., Part C: Polym. Symp. **13**, 69 (1966).
[52] M. Matsuo, M. Tamada, T. Terada, and C. Sawatari, Macromolecules **15**, 988 (1982).
[53] R. S. Stein and P. R. Wilson, J. Appl. Phys. **33**, 1914 (1962).
[54] P. Deby and A. M. Bueche, J. Appl. Phys. **20**, 518 (1949).
[55] E. Pines and W. Prins, Macromolecules **6**, 888 (1973).